Mesozoic 001 (3): 255–263
https://www.mapress.com/mz/

Article

ISSN 3021-1859 (print edition)
MESOZOIC
ISSN 3021-1867 (online edition)

https://doi.org/10.11646/mesozoic.1.3.5
http://zoobank.org/urn:lsid:zoobank.org:pub:770D413A-EF68-4279-B7D6-1E44D2B4BDF5

New age constraints for the upper Zongshan Formation: a morphometric study of the late Cretaceous orbitoidal foraminifera in Gamba area of southern Xizang (Tibet)

PEI-YUE FANG[1, *], YUE SUN[1], HUI LUO[2] & YOU-HUA ZHU[2]
[1]*School of Earth Sciences, East China University of Technology, Nanchang 330013, China*
[2]*State Key Laboratory of Palaeobiology and Petroleum Stratigraphy, Nanjing Institute of Geology and Palaeontology, CAS, Nanjing 210008, China*
pyfang7@163.com; https://orcid.org/0000-0003-0518-6222
sy0136@163.com; https://orcid.org/0000-0002-4713-049X
huiluo@nigpas.ac.cn; https://orcid.org/0000-0003-0919-4174
yhzhu@nigpas.ac.cn; https://orcid.org/0000-0001-6973-4959
**Corresponding author*

Abstract

This study refines the biostratigraphic framework of the upper Zongshan Formation in southern Xizang (Tibet) by conducting a meticulous morphometric analysis of larger benthic foraminifera (LBF) from the Gamba area. Focusing on the genera *Orbitoides* and *Omphalocyclus*, we employed a comprehensive morphometric approach to delineate the stratigraphic transition within the formation. A total of 42 samples were collected across pivotal lithological intervals, leading to the identification of species groups that provide precise age constraints for the upper Zongshan Formation. Specifically, the *O. tissoti*–*O. media* group and *Om. anatoliensis* within Limestone II to Calcareous Marl II support a late Campanian age, while the presence of the *O. megaloformis*–*O. gruenbachensis* group and potential *Om. cideensis* in Limestone III suggest a younger age bracket extending into the early Maastrichtian. Our findings not only clarify the stratigraphic position of the upper Zongshan Formation but also contribute significantly to the ongoing investigations of final evolutionary stages of the eastern Neotethys.

Keywords: LBF, Biostratigraphy, Morphometric Analysis, Zongshan Formation, Upper Cretaceous

Introduction

Upper Cretaceous strata, that is, extensive Mesozoic marine sedimentary sequences in the Neotethys Himalaya [in southern Xizang (Tibet)] represent a geological treasure trove, offering invaluable insights into Earth's history (Gansser, 1964; Wang *et al*., 1996; Yin & Harrison, 2000). The Zongshan Formation, in particular, with its rich fossil content and striking topographic rise, has emerged as a critical stratigraphic unit for understanding the Late Cretaceous paleoenvironment and bio-events (Mu *et al*., 1973; Wen, 1974). While an accurate biostratigraphic sequence is crucial for determining the precise timing of these geological events, the age constraints for the Zongshan Formation, particularly its upper part, remain an unresolved matter.

A detailed planktic foraminiferal biostratigraphic sequence for the lower Zongshan Formation (Limestone I-Calcareous Marl I) is well-established (Wan, 1985, 1987; Wan *et al*., 2000; Wendler *et al*., 2011; Fang *et al*., 2020). In contrast, the age of the upper Zongshan Formation (Limestone II-Rhodolite) has been a subject of debate. Wan (1985) assigned the upper formation to the Maastrichtian. This was followed by a broader temporal assignment from late Campanian through Maastrichtian by Wendler *et al*. (2011), and a more recent suggestion by BouDagher-Fadel *et al*. (2015) that placed it in the latest Maastrichtian. Additionally, bivalve fossils from the upper Zongshan Formation have been reported, dating to the Maastrichtian (Wen *et al*., 1976; Rao *et al*., 2012). The discrepancy in the geological age assignment of the upper Zongshan Formation is due to the absence of standardized fossil markers such as planktic foraminifera and ammonites during this period. Despite the abundance of larger benthic foraminifera in the upper Zongshan Formation, the potential of morphometric analysis as a viable and effective research tool for this group of radial foraminifera (Drooger, 1993) had been previously overlooked by those authors.

Submitted: 21 Aug. 2024; accepted by D.-Y. Huang: 13 Sept. 2024; published: 26 Sept. 2024

This study aims to address these stratigraphic ambiguities by focusing on the larger benthic foraminifera (LBF), which serve as key proxies for biostratigraphic correlation. The genera *Orbitoides* and *Omphalocyclus*, are effective bioindicators, especially in the absence of planktic foraminifera and ammonites (Caus *et al*., 1996; Özcan, 2007). Our research employs a comprehensive morphometric analysis of these two LBF genera to provide a refined chronostratigraphic framework for the upper Zongshan Formation.

Geological setting

The Himalaya can be categorized into four distinct zones from south to north: the Sub-Himalaya, Lesser Himalaya, Greater Himalaya, and Tethys Himalaya (Gansser, 1964; Wang *et al*., 1996; Yin & Harrison, 2000). To the north, the Tethyan Himalaya is demarcated by the Indus-Yarlung Zangbo Suture Zone (IYZS), and its southern boundary is defined by the Southern Tibet Detachment Surface (STDS) (Fig. 1A). Thick Mesozoic marine sedimentary strata exposed throughout the Tethyan Himalaya. During the Late Cretaceous, the Tethyan Himalaya occupied a position within the southeastern Tethys Ocean, representing a segment of the northern Indian continental plate (Fig. 1B). The Tingri-Gamba Thrust (TGT) further separates the Tethyan Himalaya into northern and southern subzones (Tapponnier *et al*., 1981; Wang *et al*., 2005; Hu *et al*., 2008) (Fig. 1A). The northern Tethyan Himalaya is

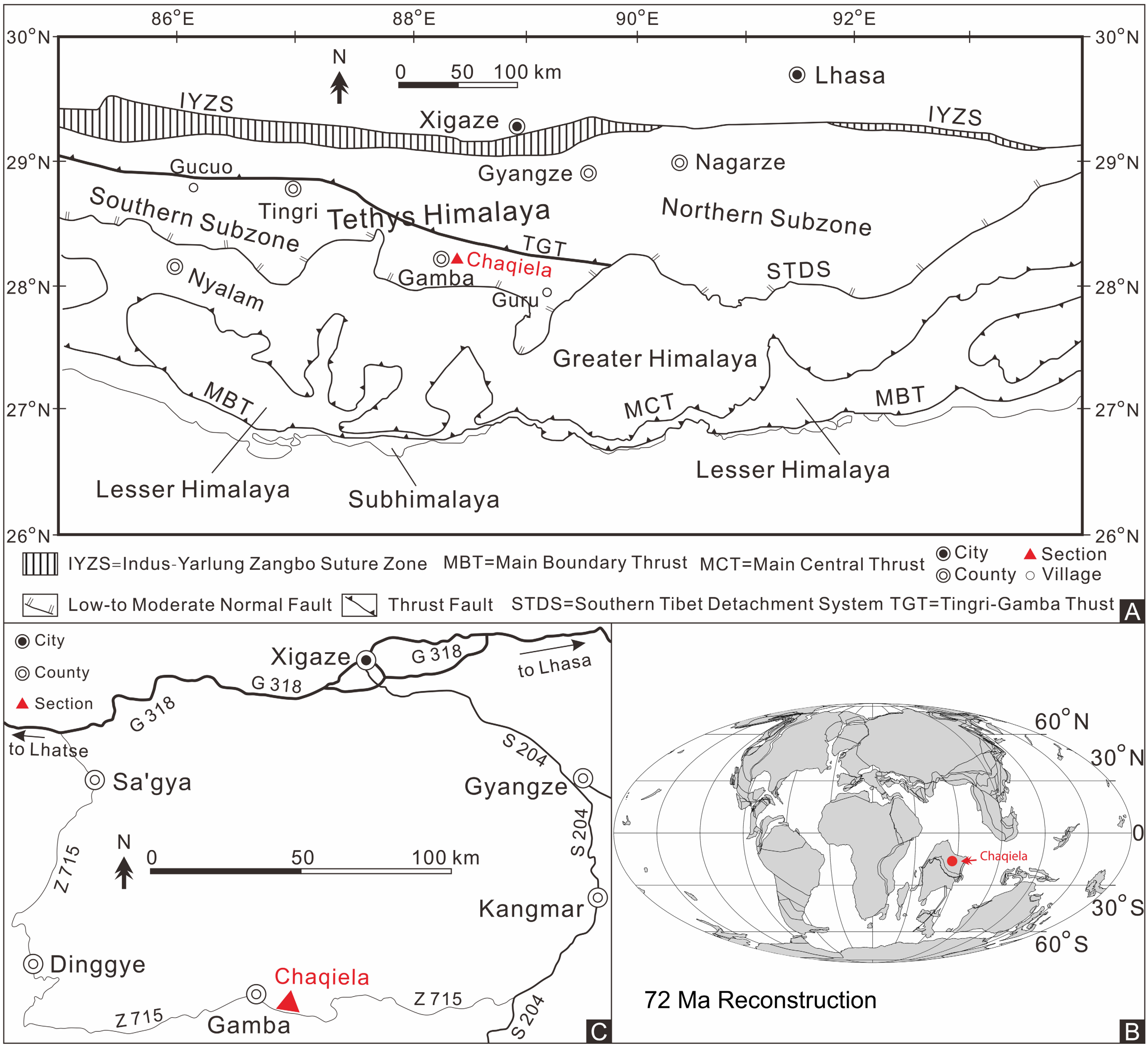

FIGURE 1. Location of the Chaqiela section in the Gamba area. **A**, Geological overview of the Chaqiela section, Gamba: tectonic framework and study area delineation (modified from Hu *et al*., 2008). **B**, Paleogeographic reconstruction for the Late Cretaceous (72 Ma) (adapted from www.odsn.de) showing the studied area. **C**, Detailed geographical map of the investigated locality and section in Gamba.

characterized by outer shelf, continental slope, and deep-water deposits (Yu & Wang, 1990; Liu & Einsele, 1994; Wang *et al*., 1996; Willems *et al*., 1996; Li *et al*., 2005; Li *et al*., 2020), whereas the southern subzone is dominated by shallow-water calcareous and terrigenous deposits (Liu & Einsele, 1994; Willems *et al*., 1996; Colpaert & Li, 2021). The studied section in the Gamba area is located in the southern Tethyan Himalaya.

In the Gamba area of southern Xizang, the Chaqiela section exposes well-preserved marine Cretaceous deposits (Wen, 1974). These strata have been classified into four lithostratigraphic units, arranged in ascending order: the Gambadongshan, the Chaqiela, the Gambacunkou, and the Zongshan formations (Mu *et al*., 1973; Wang *et al*., 1980). The Zongshan Formation, formally defined by Mu *et al*. (1973), exhibits further subdivision into three distinct limestone packages (Limestones I, II, and III), interspersed with two marly intervals (Calcareous Marls I and II), and capped by a Rhodolite member situated between Limestone III and the overlying Jidula and Zongpu formations (Fig. 2; Willems, 1993).

Material and methods

Due to severe coverage, this study has not been able to obtain samples from the Rhodolite member. All the studied samples examined in this paper were collected from the Limestone II–Limestone III of the Chaqiela section (N28°14′41.68″, E88°38′18.81″, H5054 m), about 12 km east of Gamba County (Fig. 1C). A total of 42 samples were taken with about 3.4 m spacing and several thin sections for each sample have been obtained for the LBF (Fig. 2). All illustrated specimens have been photographed using a Carl Zeiss Imager A2 at the Nanjing Institute of Geology and Palaeontology, Chinese Academy of Sciences (NIGPAS). All the studied material are housed at the NIGPAS.

For the morphometric analysis, equatorial sections were preferentially selected for their ability to clearly reveal the embryonic and peri-embryonic chamber arrangements. Terminology proposed for the genus *Orbitoides* by van Hinte (1965) and Baumfalk (1986) is also adopted for the *Omphalocyclus* due to observed

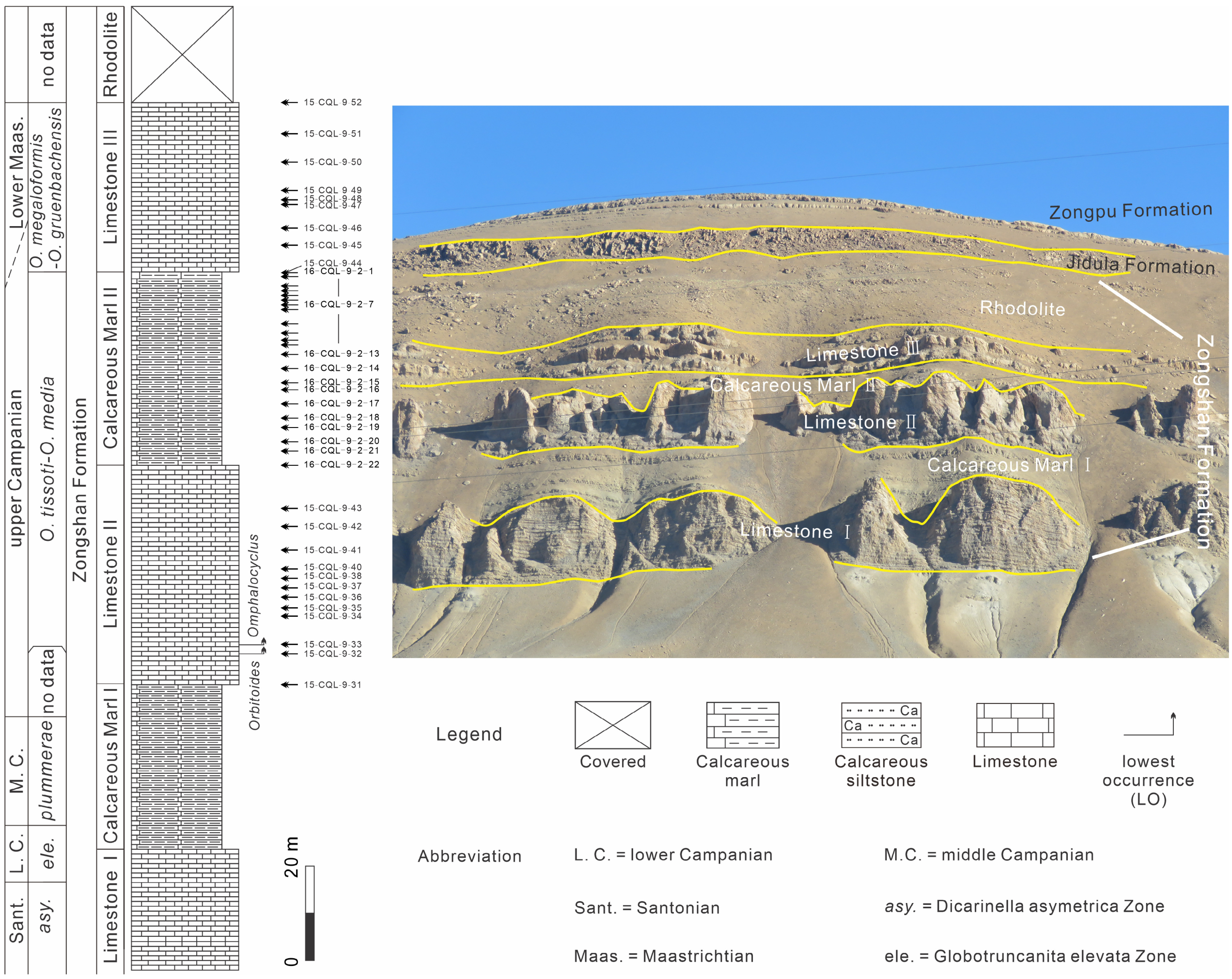

FIGURE 2. Stratigraphic column and overall view in the field of the Zongshan Formation in the Chaqiela section. Biostratigraphic data of the lower Zongshan Formation is from Fang *et al*. (2020).

structural similarities in embryonic and peri-embryonic elements (Özcan, 2007). Two key measurements (L_i and l_i in millimeters) and counts (E) were utilized to characterize the taxa, as illustrated in Fig. 3. Acknowledging the challenges associated with extracting perfect equatorial sections from solid limestone, this study also includes measurements of embryonic size from axial sections. The variability in species of *Orbitoides* and *Omphalocyclus*, based on these parameters, is comprehensively detailed in Tables 1 and 2.

Results

The upper Zongshan Formation examined in this study contains two genera of LBF: *Orbitoides* and *Omphalocyclus* (Fig. 4). The morphometric data for these genera are detailed in Tables 3 and 4, respectively.

The results indicate that, from Limestone II (samples 15-CQL-9-34 through 15-CQL-9-43) to Calcareous Marl II (samples 16-CQL-9-2-19 through 16-CQL-9-2-2), the average embryonic size (L_i+l_i) for the genus *Orbitoides* ranges from 304–502 μm, accompanied by an average of four epi-embryonic chamberlets (E), which can be classified within the *O. tissoti*–*O. media* group, indicating a late Campanian age (Caus *et al*., 1996). Regarding the genus *Omphalocyclus*, it exhibits a mean embryonic diameter (L_i+l_i) ranging from 268–404 μm, with an average of three to four epi-embryonic chamberlets (E), aligning with *Om. anatoliensis* and is also indicative of a late Campanian age (Özcan, 2007).

In Limestone III, as identified by samples 15-CQL-9-44 through 15-CQL-9-51, the mean embryonic diameter of *Orbitoides* extends from 636–784 μm. The average

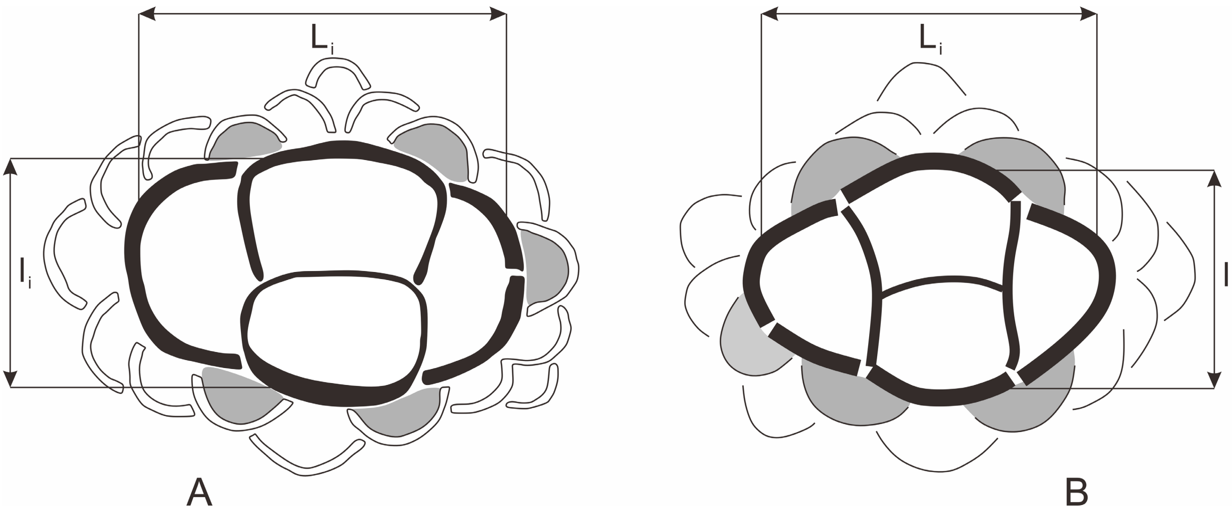

FIGURE 3. Embryonic schema and parameters including the *Orbiroides* (**A**, after Caus *et al*., 1996) and the *Omphalocyclus* (**B**, after Özcan, 2007). L_i, Largest diameter of the embryon excluding the thickness of the wall; l_i, Diameter of the embryon excluding the thickness of the wall and perpendicular to L_i; E, Total number of epi-embryonic chamberlets, with those in grey indicated.

TABLE 1. Range of variation in species of *Orbitoides* (Caus *et al*., 1996).

Species	E	L_i+l_i (μm)
O. apiculata	>14.0	>1000
O. gruenbachensis	10.0–14.0	750–1000
O. megaloformis	5.5–10.0	600–700
O. media	4.0–5.5	500–600
O. tissoti	3.9–4.0	400–500
O. douvillei	2.0–3.9	<400
O. hottingeri	0–1.0	-

TABLE 2. Range of variation in species of *Omphalocyclus* (Özcan, 2007).

Species	E	L_i+l_i (μm)
Om. anatoliensis	3–4	<480
Om. cideensis	>4	480–660
Om. macroporus	>4	>660

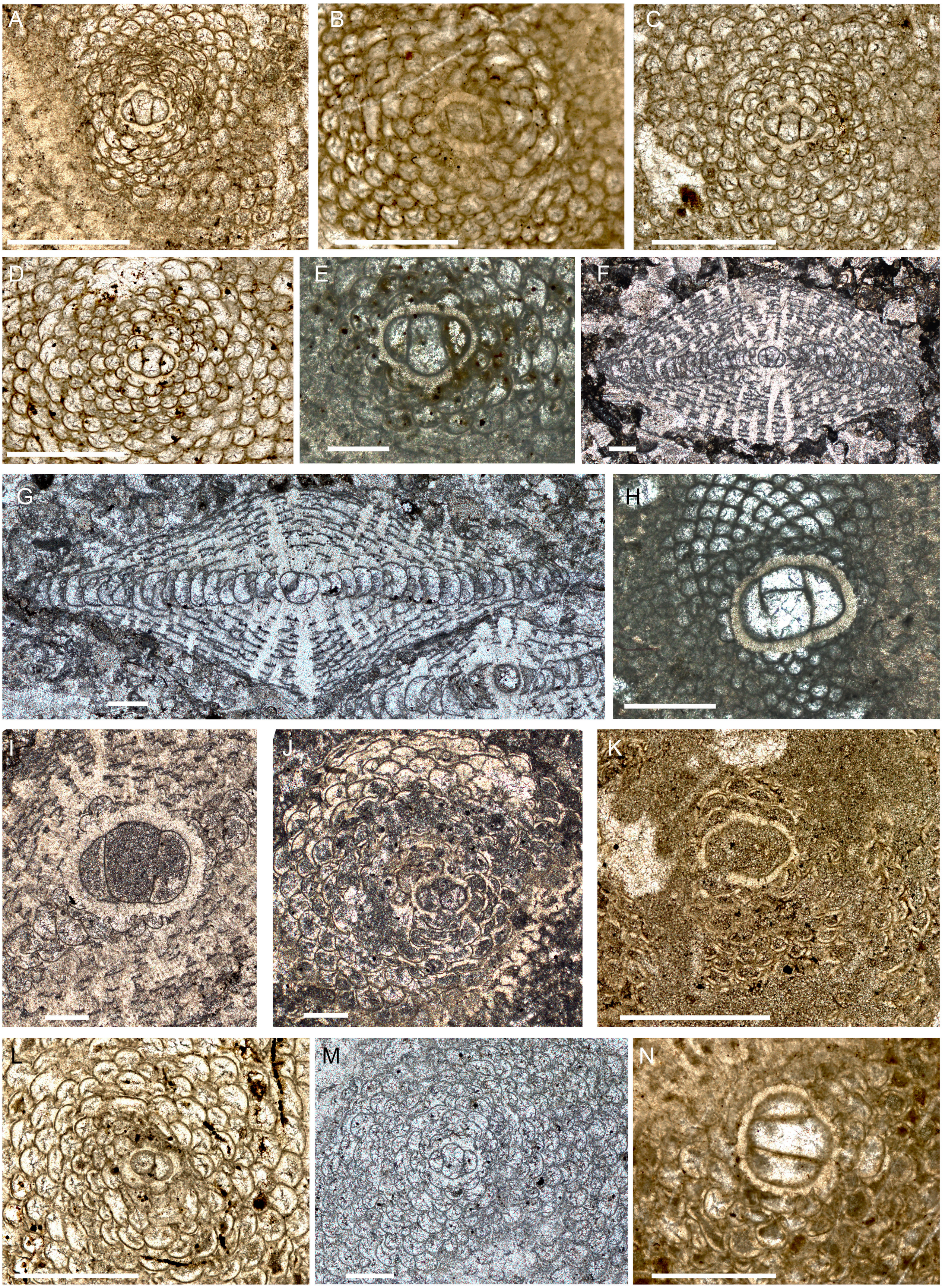

FIGURE 4. A–**G**, *O. tissoti*–*O. media* group. **A**, 15-CQL-9-34. **B**, 15-CQL-9-38. **C**, 15-CQL-9-41. **D**, 15-CQL-9-43. **E**, 16-CQL-9-2-7. **F**, 15-CQL-9-41. **G**, 16-CQL-9-2-7. **H**, **I**, *O. megaloformis*–*O. gruenbachensis* group. **H**, 15-CQL-9-44. **I**, 15-CQL-9-49. **J**–**M**, *Om. Anatoliensis*. **J**, 15-CQL-9-33. **K**, 15-CQL-9-34. **L**, 15-CQL-9-41. **M**, 16-CQL-9-2-7. **N**, *Om. cideensis*, 15-CQL-9-49. Equatorial sections: **A**–**E**, **H** and **J**–**N**; Axial sections: **F**–**G** and **I**. Sclae bars = 0.2 mm.

TABLE 3. Statistical data of *Orbitoides* populations (see the text for the abbreviations of parameters). N refers to specimen numbers. The "0" values in the "E" column indicate that the number of epi-embryonic chamberlets could not be determined due to the unavailability of suitable equatorial sections for measurement.

Samples	L_i+l_i				E			
	N	min-μm	max-μm	mean-μm	N	min	max	mean
15-CQL-9-34	5	343	440	365	2	4	4	4
15-CQL-9-37	2	422	514	468	0			
15-CQL-9-38	5	404	575	478	1	4	4	4
15-CQL-9-40	5	398	694	494	1	4	4	4
15-CQL-9-41	5	366	399	377	3	4	4	4
15-CQL-9-43	5	345	416	392	2	4	4	4
16-CQL-9-2-19	1	494	494	494	0			
16-CQL-9-2-18	1	385	385	385	0			
16-CQL-9-2-17	2	397	483	440	0			
16-CQL-9-2-16	1	380	380	380	0			
16-CQL-9-2-15	2	360	422	391	0			
16-CQL-9-2-14	1	304	304	304	0			
16-CQL-9-2-13	2	338	373	355	0			
16-CQL-9-2-10	2	298	381	340	0			
16-CQL-9-2-8	2	350	461	406	0			
16-CQL-9-2-7	4	372	662	502	0			
16-CQL-9-2-2	1	454	454	454	0			
15-CQL-9-44	3	638	991	784	0			
15-CQL-9-46	2	507	765	636	0			
15-CQL-9-49	2	565	892	729	0			

TABLE 4. Statistical data of *Omphalocyclus* populations (see the text for the abbreviations of parameters). N refers to specimen numbers.

Samples	N	*Omphalocyclus*				Species
		L_i+l_i (μm)		E		
		Range	Mean ± SE	Range	Mean ± SE	
15-CQL-9-33	4	301–438	358	3–3	3	*Om. anatoliensis*
15-CQL-9-34	3	293–474	363	3–3	3	
15-CQL-9-38	3	372–495	404	3–3	3	
15-CQL-9-41	1	285	285	3	3	
16-CQL-9-2-6	2	252–284	268	-	-	
16-CQL-9-2-7	2	308–337	323	4–4	4	
15-CQL-9-48	1	351	351			*Om. cideensis*
15-CQL-9-49	2	612–763	688			
15-CQL-9-51	1	457	457	-	-	

number of whole embryonic chambers was undetermined due to the lack of appropriate equatorial sections, yet the genus is tentatively placed within the *O. megaloformis*–*O. gruenbachensis* group, reflecting a transition from late Campanian to early Maastrichtian ages (Caus *et al.*, 1996). For *Omphalocyclus*, the mean embryon diameter varies from 351–688 μm; however, the quantification of epi-embryonic chamberlets was similarly undetermined for the same reason. Although that sample 15-CQL-9-49 exhibits an average embryonic size exceeding 660 μm, the overlying sample 15-CQL-9-51 still presents a comparatively reduced embryonic size of 457 μm. This observation has led the present study to provisionally attribute this variation to *Om. cideensis*, signifying an age bracket that spans from late Campanian to early Maastrichtian (Özcan, 2007).

Discussion

The age of the upper Zongshan Formation, notably the transition from Limestone II to the Limestone III, remains a subject of scientific debate. Wan (1985) delineated the assemblage zone characterized by the LBF genus, *Orbitoides* and *Omphalocyclus*, within this stratigraphic interval, positing a late Maastrichtian age. Subsequent research by Wendler *et al*. (2011) on the Guru section suggested a correlation between the base of Limestone II and the middle part of the planktic foraminifera *Gansserina gansseri* Zone, indicative of the Upper Campanian. Further complicating the stratigraphy, BouDagher-Fadel *et al*. (2015), in their analysis of the benthic foraminifera from the Jidula section in the Gamba region, defined the TLK 3 fossil zone by the presence of *Omphalocyclus macroporus*, thereby ascribing the upper Zongshan Formation to the latest Maastrichtian.

At the Chaqiela section, foraminifera are absent at the top of Marl I and do not appear until 6.5 meters above the base of Limestone II, where larger benthic foraminifera are first observed. The fossiliferous assemblages retrieved from the upper Zongshan Formation consist of two prominent genera of larger benthic foraminifera: *Orbitoides* and *Omphalocyclus*. In the Upper Cretaceous shallow platform settings, larger benthic foraminifera serve as effective indicators for stratigraphic correlation and division, especially when planktic foraminifera and ammonite fossils are absent. The genus *Orbitoides*, a significant bioindicator within this context, has seen the establishment of seven lineage zones through morphometric analyses (Caus *et al*., 1996). Morphometric assessments and comparisons with the species range provided by Caus *et al*. (1996) indicate that the *Orbitoides* from the Chaqiela section's Limestone II to Calcareous Marl II belong to the *O*. *tissoti*–*O*. *media* group, reflecting a late Campanian age. Meanwhile, the *Orbitoides* from Limestone III are tentatively correlated with the *O*. *megaloformis*–*O*. *gruenbachensis* evolutionary lineage, pointing towards a late Campanian to early Maastrichtian interval.

In contrast to the relatively well-documented *Orbitoides* (*e.g*., Drooger, 1993; Caus *et al*., 1996; Özcan & Özkan-Altiner, 1999), the genus *Omphalocyclus* has received less attention in the paleontological record. Historically, specimens encountered in sections were often attributed to a single species, *Omphalocyclus macroporus*, which is deemed late Maastrichtian in age. Özcan (2007) offered a refined morphometric examination of *Omphalocyclus*, proposing an evolutionary sequence from *Om*. *anatoliensis* to *Om*. *cideensis* and finally *Om*. *macroporus*. The stratigraphic distribution of *Omphalocyclus* at the Chaqiela section, as determined by morphometric data and Özcan's (2007) species delineations, suggests that specimens from Limestone II to Calcareous Marl II belong to *Om*. *anatoliensis*, indicative of late Campanian. Those from Limestone III are preliminarily assigned to *Om*. *cideensis*, marking a late Campanian to early Maastrichtian temporal bracket.

To summarize, the morphometric investigation of the benthic foraminiferal genera *Orbitoides* and *Omphalocyclus* from the Chaqiela section of the upper Zongshan Formation reveals that the strata of Limestone II to Calcareous Marl II are late Campanian in age, and the Limestone III is provisionally aligned with a period ranging from the late Campanian to the early Maastrichtian. The dimensions of the embryonic chambers and the number of epi-embryonic chamberlets within these genera are suggestive of their comparatively primitive growth stages. Collectively, these findings do not substantiate the proposition that the upper Zongshan Formation pertains to the latest Maastrichtian.

Conclusion

This study refined biostratigraphic framework for the upper Zongshan Formation in the Gamba area, southern Xizang, through the examination of larger benthic foraminifera (LBF) genera *Orbitoides* and *Omphalocyclus*. Our morphometric analysis of the genera *Orbitoides* and *Omphalocyclus* clarifies the age of the upper part of the formation, suggesting a late Campanian to early Maastrichtian transition.

The identification of the *O*. *tissoti*–*O*. *media* group and *Om*. *anatoliensis* within Limestone II to Calcareous Marl II supports a late Campanian age assignment, whereas the presence of the *O*. *megaloformis*–*O*. *gruenbachensis* group and the potential *Om*. *cideensis* in Limestone III suggests a younger age bracket extending into the early Maastrichtian. This biostratigraphic correlation offers a refined interpretation, contributing significantly to the ongoing discourse regarding the stratigraphic positioning of the upper Zongshan Formation. Our results provide an enhanced and more precise temporal framework, which is essential for a deeper understanding of the final stages of evolution in the eastern Neotethys.

Acknowledgements

This work received support from the Key Laboratory of Palaeobiology and Petroleum Stratigraphy (Nanjing Institute of Geology and Palaeontology, CAS) (No. 203104), as well as the Second Tibetan Plateau Scientific

Expedition and Research (2019QZKK0706). We are grateful to Xiting Cheng, Youdong Chen and Yang Gao of the Nanjing Institute of Geology and Palaeontology, CAS for preparing the thin sections. We are immensely grateful for Professor Özcan's guidance and assistance in the field of morphometric analysis.

References

Baumfalk, Y.A. (1986) The evolution of *Orbitoides media* (Foraminiferida) in the Late Campanian. *Journal of Foraminiferal Research*, 16 (3), 293–312. https://doi.org/10.2113/gsjfr.16.4.293

BouDagher-Fadel, M.K., Price, G.D., Hu, X.M. & Li, J. (2015) Late Cretaceous to early Paleogene foraminiferal biozones in the Tibetan Himalayas, and a pan-Tethyan foraminiferal correlation scheme. *Stratigraphy*, 12 (1), 67–91. https://doi.org/10.29041/strat.12.1.05

Caus, E., Bernaus, J.M. & Gomez-Garrido, A. (1996) Biostratigraphic utility of species of the genus *Orbitoides*. *Journal of Foraminiferal Research*, 26 (2), 124–136. https://doi.org/10.2113/gsjfr.26.2.124

Colpaert, C.P.A.M. & Li, G. (2021) Uppermost Jurassic to Lower Cretaceous benthic foraminiferal faunas of the Weimei and the Bandingsi localities of northern and southern parts of South Tibet—A preliminary analysis. *Cretaceous Research*, 124, 104785. https://doi.org/10.1016/j.cretres.2021.104785

Drooger, C.W. (1993) *Radial Foraminifera; morphometries and evolution*. North-Holland, Amsterdam, 242 pp.

Fang, P.Y., Xu, B., Mu, L., Zhu, Y.H. & Luo, H. (2020) New latest Coniacian to middle Campanian foraminiferal data from the lower Zongshan Formation in the Chaqiela section, Gamba, southern Tibet. *Palaeoworld*, 29 (1), 151–160. https://doi.org/10.1016/j.palwor.2019.05.011

Gansser, A. (1964) *Geology of the Himalayas*. *Interscience Publication John Wiley and Sons*, New York, 289 pp.

Hu, X.M., Jansa, L. & Wang, C.S. (2008) Upper Jurassic–Lower Cretaceous stratigraphy in south-eastern Tibet: a comparison with the western Himalayas. *Cretaceous Research*, 29 (3), 301–315. https://doi.org/10.1016/j.cretres.2007.05.005

Li, G., Holbourn, A., Kuhnt, W., Fang, P.Y., Yao, J.X. & Willems, H. (2020) Occurrence of benthic foraminifers across the Jurassic/Cretaceous transition in Gyangze, southern Xizang (Tibet), China. *Cretaceous Research*, 105, 103931. https://doi.org/10.1016/j.cretres.2018.08.001

Li, X.H., Wang, C.S. & Hu, X.M. (2005) Stratigraphy of deep-water Cretaceous deposits in Gyangze, southern Tibet, China. *Cretaceous Research*, 26 (4), 33–41. https://doi.org/10.1016/j.cretres.2004.11.004

Liu, G.H. & Einsele, G. (1994) Sedimentary history of the Tethyan basin in the Tibetan Himalayas. *Geologische Rundschau*, 83 (2), 32–61. https://doi.org/10.1007/BF00211893

Mu, E.Z., Yin, J.X., Wen, S.X. & Wang, Y.G. (1973) Stratigraphy of the mount Jolmo Lungma region in southern Tibet, China. *Scientia Geologica Sinica*, 1, 1–36. [In Chinese with English abstract]

Özcan, E. (2007) Morphometric analysis of the genus *Omphalocyclus* from the Late Cretaceous of Turkey: new data on its stratigraphic distribution in Mediterranean Tethys and description of two new taxa. *Cretaceous Research*, 28 (4), 621–641. https://doi.org/10.1016/j.cretres.2006.09.002

Özcan, E. & Özkan-Altiner, S. (1999) The genera *Lepidorbitoides* and *Orbitoides*: evolution and stratigraphic significance in some Anatolian basins. *Geological Journal*, 34 (3), 275–286. https://doi.org/10.1002/(SICI)1099-1034(199907/09)34:3<275::AID-GJ827>3.0.CO;2-J

Rao, X., Sha, J.G., Pan, Y.H. & Cai, H.W. (2012) Bournonia from the Late Cretaceous Zongshan Formation of Gamba, Xizang, and the functional morphology of rudist bivalves. *Acta Palaeontologica Sinica*, 51 (4), 491–501. [In Chinese with English abstract]

Tapponnier, P., Mercier, J.L., Proust, F., Andrieux, J., Armijo, R., Bassoullet, J.P., Brunel, M., Burg, J.P., Colchen, M., Dupré, B., Girardeau, J., Marcoux, J., Mascle, G., Matte, P., Nicolas, A., Li, T., Xiao, X., Chang, C., Lin, P., Li, G., Wang, N., Chen, G., Han, T., Wang, X., Den, W., Zhen, H., Sheng, H., Cao, Y., Zhou, J. & Qiu, H. (1981) The Tibetan side of the India—Eurasia collision. *Nature*, 294 (3), 405–410. https://doi.org/10.1038/294405a0

Van Hinte, J.E. (1965) An approach to *Orbitoides*. *Proceedings of the Koninklijke Nederlandse Akademie van Wetenschappen*, 68, 57–70.

Wan, X.Q. (1985) Cretaceous strata and Foraminifera of Gangba region, Xizang. *Contribution to the geology of the Qinghai-Xizang (Tibet) Plateau*, 16, 203–228. [In Chinese with English abstract]

Wan, X.Q. (1987) Cretaceous planktonic foraminifera zonation in Xizang (Tibet). *Contribution to the geology of the Qinghai-Xizang (Tibet) Plateau*, 18, 112–121. [In Chinese with English abstract]

Wan, X.Q., Zhao, W.J. & Li, G.B. (2000) Restudy of the Upper Cretaceous in Gamba, Tibet. *Geoscience*, 14 (3), 281–285. [In Chinese with English abstract]

Wang, C.S., Li, X.H., Hu, X.M., Wan, X.Q., Yin, J.R., Huang, Y.J., Huang, S.J. & Li, G.B. (2005) *Sedimentary Geology and Continental Paleoceanography in Tethyan Himalayas*. Geological Publishing House, Beijing, 373 pp. [In Chinese with English abstract]

Wang, C.S., Xia, D.X., Zhou, X., Chen, J.P., Lu, Y., Wang, G.H., He, Z.W., Li, X.H., Wan, X.Q., Zeng, Q.G., Pubu, C. & Liu, Z.F. (1996) *Field Trip Guide T121/T387, Geology between the Indus-Yarlung Zangbo Suture Zone and the Himalaya Mountains, Xizang (Tibet), China*. Geological Publishing House, Beijing, 72 pp.

Wang, Y.G., Sun, D.L. & He, G.X. (1980) New advances in the stratigraphy of the Chinese part of the Himalayas. *Journal of Stratigraphy*, 4 (1), 55–59. [In Chinese]

Wen, S.X. (1974) Stratigraphy of the Mount Jolmo Lungma region: Cretaceous. *In*: Comprehensive Scientific Expedition Team to Xizang, Chinese Academy of Sciences (Ed.), *A Report of the Scientific Expedition in the Mount Jolmo Lungma Region (1966–1968), Geology*. *Science Press*, Beijing, pp. 148–183. [In Chinese]

Wen, S.X., Lan, X., Chen, J.H., Zhang, Z.M., Chen, C.Z. & Gu, Z.W. (1976) Fossil Lamellibranchia from the Mount Jolmo Lungma region. *In*: Comprehensive Scientific Expedition to Xizang, Chinese Academy of Sciences (Eds), *A Report of the Scientific Expedition in the Mount Jolmo Lungma Region (1966–1968), Paleontology (3)*. Scientific Press, Beijing, pp. 1–210. [In Chinese]

Wendler, I., Willems, H., Gräfe, K.U., Ding, L. & Luo, H. (2011) Upper Cretaceous inter-hemispheric correlation between the Southern Tethys and the Boreal: chemo-and biostratigraphy and paleoclimatic reconstructions from a new section in the Tethys Himalaya, S-Tibet. *Newsletters on Stratigraphy*, 44 (2), 137–171. https://doi.org/10.1127/0078-0421/2011/0010

Willems, H. (1993) *Geoscientific investigations in the Tethyan Himalayas*. Fachbereich Geowissenschaften der Universität Bremen, 183 pp.

Willems, H., Zhou, Z., Zhang, B. & Gräfe, K.U. (1996) Stratigraphy of the Upper Cretaceous and Lower Tertiary strata in the Tethyan Himalayas of Tibet (Tingri area, China). *Geologische Rundschau*, 85 (3), 723–754. https://doi.org/10.1007/s005310050108

Yin, A. & Harrison, T.M. (2000) Geologic evolution of the Himalayan-Tibetan orogen. *Annual Review of Earth and Planetary Sciences*, 28 (1), 211–280. https://doi.org/10.1146/annurev.earth.28.1.211

Yu, G.M. & Wang, C.S. (1990) *Sedimentary geology of the Xizang (Tibet) Tethys*. Geological Publishing House, Beijing, 185 pp. [In Chinese with English abstract]